

# Nanosheet Formation in Hyperswollen Lyotropic Lamellar Phases

Yoshiaki Uchida,<sup>\*,†,‡</sup> Takuma Nishizawa,<sup>†</sup> Takeru Omiya,<sup>†</sup> Yuichiro Hirota,<sup>†</sup> and Norikazu Nishiyama<sup>†</sup>

<sup>†</sup>Graduate School of Engineering Science, Osaka University, 1-3 Machikaneyama-cho, Toyonaka, Osaka 560-8531, Japan

<sup>‡</sup>PRESTO, Japan Science and Technology Agency (JST), Kawaguchi, Saitama 332-0012, Japan

## Supporting Information

**ABSTRACT:** Nanosheets ( $\sim 1$  nm) are formed using a nonionic hyperswollen lyotropic lamellar phase as a template. The accumulation and reaction of ingredients in the highly separated (several hundred nm) bilayers in the hyperswollen lyotropic lamellar phase should result in very thin nanosheets. This method could be applied to the synthesis of a wide variety of two-dimensional organic and inorganic materials.

Surfaces and interfaces of materials show unique chemical and physical properties extremely different from bulk properties of the same materials. As materials with only surfaces, nanoparticles, nanowires, and nanosheets are promising materials showing fascinating properties. In particular, nanosheets with exceptionally small thickness exhibit possible quantum size effects;<sup>1–4</sup> carbonaceous nanosheets like graphene and graphene oxide,<sup>1</sup> and nanosheets consisting of metals like Au<sup>5</sup> and Ni,<sup>6</sup> semiconductors like ZnS<sup>7</sup> and TiO<sub>2</sub>,<sup>8</sup> and metal oxides like WO<sub>3</sub><sup>9</sup> and MgO<sup>10</sup> have been reported. The synthetic protocols of nanosheets are divided into two categories: top-down exfoliation methods, and bottom-up methods like chemical vapor deposition and hydrothermal synthesis.<sup>1–3</sup> Since the first nanosheet was obtained from the exfoliation of a natural layered material, smectite,<sup>4</sup> variable nanosheets of intrinsically layered materials have been fabricated by the top-down exfoliation methods. Meanwhile, the bottom-up two-dimensional (2-D) growth on a smooth substrate has recently been used to obtain nanosheets of nonlayered materials. Recently, an improved bottom-up method using ordinary lyotropic lamellar phase has been reported,<sup>11</sup> which concentrated amphiphile solutions often show. However, materials tend to form thick (several tens nm) nanosheets due to the high concentration of the ingredients and the close contacts between adjacent nanosheets. More separated 2-D templates are necessary to obtain very thin nanosheets of nonlayered materials. The highly separated nanosheets should also be advantageous to the next adsorption process.<sup>14,15</sup> In some suspensions of nanosheets, e.g., graphene oxide<sup>12</sup> and H<sub>3</sub>Sb<sub>3</sub>P<sub>2</sub>O<sub>14</sub>,<sup>13</sup> nanosheets are known to be periodically separated with the separation of tens or hundreds of nanometers. This structure resembles to one of lyotropic liquid crystalline phases.

Hyperswollen lyotropic lamellar phases consist of amphiphilic bilayers periodically separated by several hundreds of nanometer as shown in Figure 1a, which causes selective reflection. The accumulation and reaction of ingredients in the highly separated (several hundred nanometers) bilayers in the hyperswollen lyotropic lamellar phase should result in very thin nanosheets.

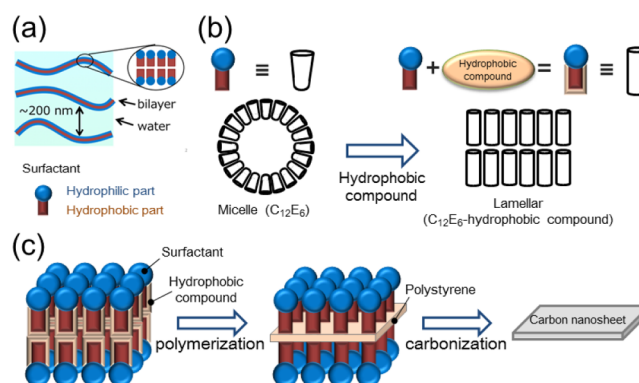


**Figure 1.** Stabilization mechanisms of hyperswollen lamellar phase and synthetic procedure of nanosheets. (a) Hyperswollen lamellar phases have highly separated ( $\sim 200$  nm for aqueous  $C_{12}E_6$  solutions) bilayers. (b) Aqueous  $C_{12}E_6$  solutions naturally do not show any hyperswollen lamellar phases due to the packing parameter of  $C_{12}E_6$ . When a hydrophobic compound is introduced in a  $C_{12}E_6$  solution, the hydrophobic part of self-assembly structures practically increases. As a result, the hyperswollen lamellar phase is stabilized. (c) In the polymerization process, the monomer is stacked in the bilayers of the hyperswollen lamellar phase. After spin-coating on a silicon substrate, the polymer nanosheets are carbonized in  $N_2$  atmosphere for 5 h at  $800$  °C with heating rate of  $1$  °C/min.

This orientational ordering of the nanosheets is desirable for highly controlled adsorption; this adsorption process would enable us to directly prepare the one layer adsorption of fresh nanosheets. This extraordinary lamellar phase is stabilized even for nonionic amphiphile solutions by undulation of the layers, Helfrich interaction, which keeps the layer spacing.<sup>16</sup> The investigation of the synthesis of nanosheet materials in the hyperswollen lamellar phases of nonionic amphiphile solutions would give us the information how Helfrich interaction works. This information is not only technologically useful for the synthesis of various nanosheet materials but also scientifically important because Helfrich interaction is believed to commonly stabilize layered phases. To clarify the mechanism, we focus on the synthesis of the soft polymer nanosheets, precursors for carbon nanosheets, in the thin hydrophobic part of the bilayers. The softness of the nanosheets in the bilayers would not diminish the undulation.

As the amphiphile, we select nonionic polyethylene glycol monoalkyl ether ( $C_mE_n$ ;  $m$  is the alkyl carbon number, and  $n$  is the number of the ethylene glycol units). In general, the volume

Received: October 30, 2015

Published: January 25, 2016

ratio between the hydrophobic and hydrophilic parts of the amphiphile, packing parameter, is important to show hyperswollen lyotropic lamellar phases. In fact, the ratio of  $m/n$  determines the phase transition behaviors; hyperswollen lyotropic lamellar phases appear when  $m/n$  is in a certain range (2.4–4). For example, the aqueous solutions of  $C_{12}E_5$  and  $C_{10}E_4$  show hyperswollen lyotropic lamellar phases, whereas those of  $C_{12}E_6$  and  $C_{10}E_3$  do not. This situation drastically changes, provided that third component is added to the amphiphile solution. When  $C_{12}E_8$  aqueous solution, which does not exhibit any hyperswollen lyotropic lamellar phases intrinsically, is doped with 1-hexanol, the solution shows hyperswollen lyotropic lamellar phases because the hydrophobic part swells<sup>17</sup> as shown in Figure 1b. If the hydrophobic additive is changed to polymerizable monomer, polymer nanosheets could be synthesized as shown in Figure 1c. Since aromatic monomers are suitable for the precursor polymer of carbon nanosheets, we employed styrene as the simplest monomer meeting the requirement, and if the addition of the monomer to an amphiphile solution not showing hyperswollen lyotropic lamellar phases intrinsically induces hyperswollen lamellar phase, we could say that the monomer stabilizes the hyperswollen lamellar phase. This protocol would enable us to check if the monomer forms nanosheet aggregate. Thus,  $C_{12}E_6$  is suitable as such an amphiphile to obtain carbon nanosheets as thin as possible; its  $m/n$  is 2.0 close to the lower limit of  $m/n$  for showing hyperswollen lamellar phases (2.4). Here we show that the synthesis of polymer nanosheets forms in the hyperswollen lamellar phase of  $C_{12}E_6$  solution with styrene, which serves as a printable or coatable precursor for carbon nanosheets.

First, we examined whether aqueous  $C_{12}E_6$  solution added the model nonpolymerizable compound of styrene shows a hyperswollen lyotropic lamellar phase in detail. As the model additive, we used toluene with similar structure to styrene. We prepared a solution of  $C_{12}E_6$  with toluene by gently shaking them in water. The mass ratio of  $C_{12}E_6$  and toluene is 5:1. Obtained solution gave blue color due to their light scattering. The hyperswollen lyotropic lamellar phases of  $C_mE_n$  solutions are induced by sheering, stirring, or flowing of the solution. In fact, after stirring the solution, iridescent colors emerge; this is typical of hyperswollen lamellar phases.<sup>18</sup> The aqueous solutions of  $C_{12}E_6$  and toluene with the concentration between 1.2 and 2.0 wt % show hyperswollen lamellar phases between 42 and 58 °C. To confirm whether the aqueous solution of  $C_{12}E_6$  and toluene shows hyperswollen lyotropic lamellar phases, we measured reflectance spectra according to ref 19 with experimental setup shown in Figure 2a. The reflectance spectra depend on the concentration of the solutes as shown in Figure 2b because the selective reflection peak was shifted to longer wavelength and its corresponding layer spacing, which can be calculated by the Bragg equation shown in the Supporting Information, elongates from 210 to 260 nm as concentration decreases from 2.0 to 1.2 wt %.

We synthesized polymer nanosheets in the hyperswollen lamellar phase by replacing toluene of the above-mentioned aqueous  $C_{12}E_6$ –toluene solutions with polymerizable styrene. The  $C_{12}E_6$ –styrene system exhibits hyperswollen lamellar phases with wide range of concentration like  $C_{12}E_6$ –toluene system. To polymerize styrene in the temperature range of the hyperswollen lamellar phase (42–58 °C), the appropriate concentration of hydrophobic polymerization initiator was needed.<sup>20</sup> The polymerization inhibitor in styrene was removed by washing styrene with 0.1 M NaOH solution and deionized water. The

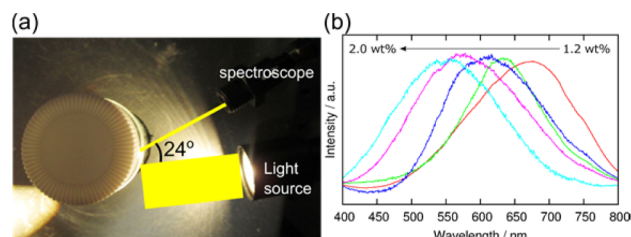


**Figure 2.** Reflectance spectroscopy of  $C_{12}E_6$  solution. (a) Experimental setup for the reflectance spectroscopy. To remove scattering light as much as possible, the incident light is off-central to the vial and the reflected light at  $2\theta = 24^\circ$  is detected. (b) Reflectance spectra for  $C_{12}E_6$  solutions with various concentrations. The spectra were differential spectra between the spectra of a sample stirred at 300 rpm and those of the same sample unstirred. Thus, the intensities of the different samples are incomparable with each other.

resulted styrene (0.3 mL) and polymerization initiator 2,2'-azobis(isobutyronitrile) (AIBN, 0.01 g) were mixed.  $C_{12}E_6$  (0.09 g) and the styrene–AIBN mixture (0.03 g) were dissolved in deionized water (4.38 g). The solution was stirred at 300 rpm by a stir bar with length of 20 mm and diameter of 7 mm at 54 °C for 24 h. During the polymerization process, the solution keeps showing iridescent colors, which are typical of hyperswollen lamellar phases.<sup>18</sup> It suggests that the polymerization does not inhibit the hyperswollen lamellar phase; the resulted polymer is soft enough to keep the undulation of the bilayers. The solution was applied on a silicon substrate, and the substrate was carbonized as shown in Figure 1c.

We observe the obtained carbonaceous materials on the silicon substrate by TEM and AFM. Some TEM images demonstrate that carbon nanosheets are generated on the silicon substrates as shown in Figure 3a. In contrast, when the amount of the

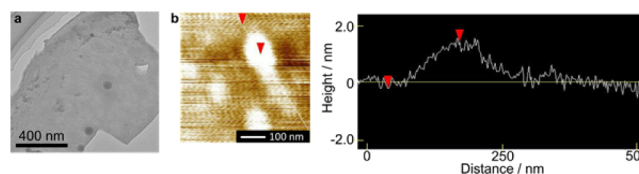


**Figure 3.** Synthesized carbon nanosheets. (a) TEM photograph of one of the synthesized carbon nanosheets. (b) AFM photograph and cross section of one of the synthesized carbon nanosheets. These indicate that the thickness and horizontal width of the synthesized carbon nanosheets are a few nanometers and several hundred nanometers, respectively.

ingredients is in excess, the height of the products becomes not uniform as shown in Figure S1. In the hyperswollen lamellar phase of the  $C_{12}E_6$ –styrene aqueous solution, styrene is accumulated in the hydrophobic region of the bilayers. Sheeted polystyrene is formed in the bilayers, and the polystyrene is carbonized to carbon nanosheets. The thickness and horizontal width of the carbon nanosheets measured by AFM are a few nanometers and several hundred nanometers, respectively, as shown in Figures 3b and S2 (the aspect ratio is about 100). These results indicate that the bilayer-template method using hyperswollen lamellar phase of nonionic amphiphile enables us to synthesize sheeted polymer and to produce carbon nanosheets on a silicon substrate.

To apply this method to a wide range of materials, reaction temperature is needed to be controllable. Helfrich interaction depends on the viscosity of the aqueous phase of the hyperswollen lamellar phase; the more the viscosity increases,

the more the temperature range is expected to decrease. Thus, we tried to add glycerin to the  $C_{12}E_5$  aqueous solution with the concentration showing a hyperswollen lamellar phase. The  $C_{12}E_5$ -glycerin system also shows iridescent colors characteristic of hyperswollen lamellar phases.<sup>18</sup> As anticipated, the higher the glycerin concentration, the lower the temperature range of the hyperswollen lamellar phases, as shown in Figure 4.

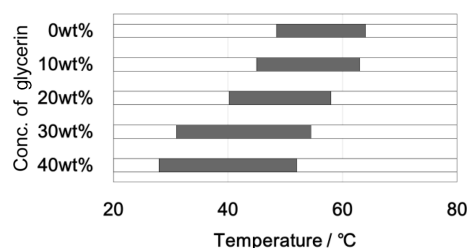


**Figure 4.** Phase transition behavior of aqueous  $C_{12}E_5$  solution with glycerin. The phase transition temperatures of the hyperswollen lamellar phases depend on the concentration of glycerin. The higher the concentration of glycerin, the lower the temperature of the hyperswollen lamellar phase and the wider the temperature range.

In summary, we have succeeded the synthesis of polymer nanosheets in hyperswollen lyotropic lamellar phases, which also can be ingredients of carbon nanosheets. Since the amount of the monomer the bilayers of hyperswollen lamellar phase can hold is limited, the thickness of the resulted nanosheets is almost constant. Since we also found the temperature of the phase can be controlled by the addition of glycerin, this method is applicable to the synthesis of a wide range of materials, for which reaction temperature differs depending on materials. Furthermore, the nanosheets formed in the bilayers are dispersed in the aqueous solution from the beginning. This is highly desirable to the adsorption of the nanosheets on substrates. Since disparate nanosheets can be synthesized in the same phase, alternating stacking with desired combination would be easily realized. In addition, since the hyperswollen phase is stabilized not by Coulombic interaction but by Helfrich interaction,<sup>16</sup> the bilayers are not easily perturbed by ionic contaminations, and thus, the nonionic amphiphile solution system is favorable for the preparation of ionic nanosheets as well as nonionic nanosheets. Thus, various hydrophobic nanosheets could be formed in the bilayers by changing the ingredients: 2-D organic crystals and 2-D MOFs. Especially, the latter should show extraordinary absorption behaviors different from those of bulk MOFs.<sup>21</sup> Meanwhile, hyperswollen lamellar phases of organic solutions of ionic amphiphiles might be applicable to the synthesis of hydrophilic nanosheets: titanate nanosheets<sup>22</sup> and iron oxide nanosheets.<sup>23</sup>

## ■ ASSOCIATED CONTENT

### Supporting Information

The Supporting Information is available free of charge on the ACS Publications website at DOI: 10.1021/jacs.5b11256.

Derivation of layer spacings and TEM and AFM photographs; Figures S1–2 (PDF)

## ■ AUTHOR INFORMATION

### Corresponding Author

\*yuchida@cheng.es.osaka-u.ac.jp

## Notes

The authors declare no competing financial interest.

## ■ ACKNOWLEDGMENTS

This work was supported in part by the Japan Science and Technology Agency (JST) “Precursory Research for Embryonic Science and Technology (PRESTO)” for a project of “Molecular technology and creation of new function”, and the Grant-in-Aid for Scientific Research (No. 25289228 and 25610123) from Japan Society for the Promotion of Science (JSPS). We thank Professor Jun Yamamoto and Dr. Yoshiyuki Komoda for helpful advices. The TEM measurements were carried out by using a facility in the Research Center for Ultrahigh Voltage Electron Microscopy, Osaka University.

## ■ REFERENCES

- (1) Rao, C. N. R.; Ramakrishna Matte, H. S. S.; Maitra, U. *Angew. Chem., Int. Ed.* **2013**, *52*, 13162–13185.
- (2) Ma, R.; Sasaki, T. *Adv. Mater.* **2010**, *22*, 5082–5104.
- (3) Liu, Y.; Wu, Z.; Zhang, H. *Adv. Colloid Interface Sci.* **2014**, *207*, 347–360.
- (4) MacEwan, D. M. C.; Wilson, M. J. In *Crystal Structures of Clay Minerals and Their X-ray Identification*; Brindley, G. W., Brown, G., Eds.; Mineralogical Society of Great Britain and Ireland: Middlesex, United Kingdom, 1980; Chapter 3, p 197.
- (5) Sanyal, A.; Murali, S. *Chem. Commun.* **2003**, 1236–1237.
- (6) Liang, Z.-H.; Zhu, Y.-J.; Hu, X.-H. *J. Phys. Chem. B* **2004**, *108*, 3488–3491.
- (7) Fang, X.-S.; Ye, C.-H.; Zhang, L.-D.; Wang, Y.-H.; Wu, Y.-C. *Adv. Funct. Mater.* **2005**, *15*, 63–68.
- (8) Moriguchi, I.; Maeda, H.; Teraoka, Y.; Kagawa, S. *J. Am. Chem. Soc.* **1995**, *117*, 1139–1140.
- (9) Choi, H. G.; Jung, Y. H.; Kim, D. K. *J. Am. Ceram. Soc.* **2005**, *88*, 1684–1686.
- (10) Yan, C.; Xue, D. *J. Phys. Chem. B* **2005**, *109*, 12358–12361.
- (11) Min, Y.; Moon, G. D.; Kim, C.-E.; Lee, J.-H.; Yang, H.; Soon, A.; Jeong, U. *J. Mater. Chem. C* **2014**, *2*, 6222–6248.
- (12) Xu, Z.; Gao, C. *ACS Nano* **2011**, *5*, 2908–2915.
- (13) Gabriel, J.-C. P.; Camerel, F.; Lemaire, B. J.; Desvaux, H.; Davidson, P.; Batail, P. *Nature* **2001**, *413*, 504–508.
- (14) Keller, S. W.; Kim, H.-N.; Mallouk, T. E. *J. Am. Chem. Soc.* **1994**, *116*, 8817–8818.
- (15) Kleinfeld, E. R.; Ferguson, G. S. *Science* **1994**, *265*, 370–373.
- (16) Helfrich, W. *Z. Naturforsch., A: Phys. Sci.* **1978**, *33a*, 305–315.
- (17) Strey, R.; Schomacker, R.; Roux, D.; Nallet, F.; Olsson, U. *J. Chem. Soc., Faraday Trans.* **1990**, *86*, 2253–2261.
- (18) Yamamoto, T.; Satoh, N.; Onda, T.; Tsujii, K. *Langmuir* **1996**, *12*, 3143–3150.
- (19) Kobayashi, C.; Yamamoto, J.; Takanishi, Y. *J. Appl. Phys.* **2012**, *112*, 013531.
- (20) Holland, B. T.; Blanford, C. F.; Do, T.; Stein, A. *Chem. Mater.* **1999**, *11*, 795–805.
- (21) Sakata, Y.; Furukawa, S.; Kitagawa, S. *Science* **2013**, *339*, 193–196.
- (22) Sugimoto, W.; Terabayashi, O.; Murakami, Y.; Takasu, Y. *J. Mater. Chem.* **2002**, *12*, 3814–3818.
- (23) Tsujimoto, Y.; Tassel, C.; Hayashi, N.; Watanabe, T.; Kageyama, H.; Yoshimura, K.; Takano, M.; Ceretti, M.; Ritter, C.; Paulus, W. *Nature* **2007**, *450*, 1062–1065.